On the study of catalytic membrane reactor for water detritiation: Modeling approach

Karine Liger, Jérémy Mascarade, Xavier Joulia, Xuan Mi Meyer, Michèle Troulay, Christophe Perrais

On the study of catalytic membrane reactor for water detritiation: Modeling approach

Karine Liger[a,*], Jérémy Mascarade[a], Xavier Joulia[b,c], Xuan-Mi Meyer[b,c], Michèle Troulay[a], Christophe Perrais[a]

[a] CEA, DEN, DTN/SMTA/LIPC Cadarache, Saint Paul-lez-Durance F-13108, France
[b] Université de Toulouse, INPT, UPS, Laboratoire de Génie Chimique, 4, Allée Emile Monso, Toulouse F-31030, France
[c] CNRS, Laboratoire de Génie Chimique, Toulouse F-31030, France

- Experimental results for the conversion of tritiated water (using deuterium as a simulant of tritium) by means of a catalytic membrane reactor in view of tritium recovery.
- Phenomenological 2D model to represent catalytic membrane reactor behavior including the determination of the compositions of gaseous effluents.
- Good agreement between the simulation results and experimental measurements performed on the dedicated facility.
- Explanation of the unexpected behavior of the catalytic membrane reactor by the modeling results and in particular the gas composition estimation.

In the framework of tritium recovery from tritiated water, efficiency of packed bed membrane reactors have been successfully demonstrated. Thanks to protium isotope swamping, tritium bonded water can be recovered under the valuable Q_2 form ($Q = H$, D or T) by means of isotope exchange reactions occurring on catalyst surface. The use of permselective Pd-based membrane allows withdrawal of reactions products all along the reactor, and thus limits reverse reaction rate to the benefit of the direct one (shift effect). The reactions kinetics, which are still little known or unknown, are generally assumed to be largely greater than the permeation ones so that thermodynamic equilibriums of isotope exchange reactions are generally assumed. This paper proposes a new phenomenological 2D model to represent catalytic membrane reactor behavior with the determination of gas effluents compositions. A good agreement was obtained between the simulation results and experimental measurements performed on a dedicated facility. Furthermore, the gas composition estimation permits to interpret unexpected behavior of the catalytic membrane reactor. In the next future, further sensitivity analysis will be performed to determine the limits of the model and a kinetics study will be conducted to assess the thermodynamic equilibrium of reactions.

1. Introduction

During its lifecycle, a *D–T* fusion machine will produce amounts of tritiated waste of various activities and natures [1]. Several issues associated to tritiated waste management have been pointed out since 1997 as a result of the DTE1 experiments done in the JET machine [2]. Thus, for economic and environmental reasons, several processes have been developed since decades either to recover volatile tritiated species (Q_2 and/or Q_2O where $Q = H$, D or T) as fusion fuel or to trap them by for instance oxidation/adsorption processes [3].

A promising intensified process considered for the recovery of tritium uses combined effects of catalytic conversion and selective membrane purification properties. Even though efficiency of such a process has already been demonstrated either on soft housekeeping waste [4] or highly tritiated water effluents [5], some mechanisms, particularly in terms of reaction conversions are not really well known yet. Considering deuterium as tritium tracer, the overall set of reactions occurring with a Q_2/Q_2O mixture is given below:

$$D_2O + H_2 \rightleftharpoons HDO + HD \quad (R1)$$

$$HDO + H_2 \rightleftharpoons H_2O + HD \quad (R2)$$

$$H_2 + D_2 \rightleftharpoons 2 \times HD \quad (R3)$$

$$D_2O + H_2 \rightleftharpoons H_2O + D_2 \quad (R4)$$

$$HDO + D_2 \rightleftharpoons D_2O + HD \quad (R5)$$

$$H_2O + D_2 \rightleftharpoons HDO + HD \quad (R6)$$

$$2HDO \rightleftharpoons H_2O + D_2O \quad (R7)$$

From the above reversible reaction set, two possible chemical pathways appear: if reactions' thermodynamic equilibriums are reached, (R1)–(R3) reactions are sufficient to describe the whole system. Indeed, (R4)–(R7) equilibrium constants are linear combinations of the three others. Nevertheless, if chemical reacting system is rate limited, kinetics of each of the 7 reactions must be considered. Considering the fact that above a temperature of nearly 100 °C reactions (R1)–(R3) have reached their thermodynamic equilibriums, most of catalytic membrane reactor models have neglected the reactions kinetics [6–8]. Based on this assumption, a new phenomenological model is proposed including gaseous effluents speciation. Results of this model are compared to experimental results obtained on a dedicated facility.

2. Experimental facility

An experimental test bench has been built at CEA Cadarache to perform parametric study on catalytic membrane reactors. Fig. 1 gives a schematic view of the instrumented experimental device; a detailed description of the process has already been reported [9]. Diluted deuterated feed stream, composed of binary mixtures of N_2 and D_2O, is fed to the lumen side of a finger-type catalytic membrane reactor containing about 20 g of commercial Ni-Based catalyst pellets (NiSAT® 310RSCDS). The membrane tube (length = 48.5 cm, outer diameter = 1 cm, wall thickness = 150 μm) is made of a defect free $Pd_{77}Ag_{23}$ alloy allowing only hydrogen isotopes permeation. The feed stream reacts with permeated protium coming from the counter-current sweep stream. Deuterium hydride and dideuterium produced are partially removed from the lumen side by counterdiffusion through the membrane and withdrawn by the permeate stream. Remaining reaction products are removed by the retentate stream.

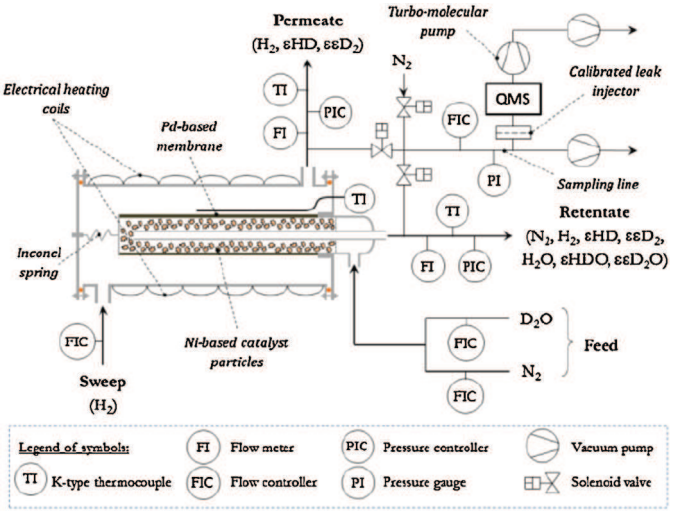

Fig. 1. Detailed instrumentation plan of the facility.

Calibration of the analysis chain is described in [9]. Combining the composition measurements with the streams total flow rates allowed to track molecular and atomic species from any inlet to any outlet of the catalytic membrane reactor. Because of measurement errors and to compare measured and calculated values, data reconciliation on raw measurements results was done. A maximal deviation of 7% was encountered between raw and reconciled measurements.

3. Modeling approach

The design of the catalytic membrane reactor permits to define 2 zones (the lumen and the shell) to be considered for the mass balance, both zones being separated by the membrane in through which permeation occurs. Considering that:

- the profiles along the reactor's centerline are axis-symmetric ($\partial/\partial\theta = 0$);
- the entire module is isothermal ($\partial/\partial T = 0$);
- the lumen's pressure-drop can be neglected;
- the thermodynamic behavior is described by ideal gas equation of state and the gas is assumed to be incompressible;
- the membrane is defect free (infinite selectivity toward protium and deuterium);
- the chemical reactions occur at the catalyst surface and thermodynamic equilibrium is assumed at any point of the lumen;
- the catalyst is assumed to be composed of monodisperse cylindrical particles.

Then, for each species i, the mass balance can be written for the lumen and the shell sides.

3.1. Mass balance in the lumen

For each species i, the mass balance is represented in the gas phase by:

$$\varepsilon\frac{\partial C_i^{\text{lumen}}}{\partial t} - u_r\frac{\partial C_i^{\text{lumen}}}{\partial r} + u_z\frac{\partial C_i^{\text{lumen}}}{\partial z} = \varepsilon\frac{\partial}{\partial z}\left(\mathcal{D}_{\text{ax},i}\frac{\partial C_i^{\text{lumen}}}{\partial z}\right) + \frac{1}{r}\frac{\partial}{\partial r}\left(\varepsilon\mathcal{D}_{\text{rad},i}\frac{\partial C_i^{\text{lumen}}}{\partial r}\right) - k_{g,i}a_v\left(C_i^{\text{lumen}} - C_i^*\right) \quad (1)$$

where C_i^{lumen} is the concentration of species i in the lumen (mol/m^3), ε is the fixed bed porosity (−), u_r and u_z are, respectively, the radial and axial velocity (m/s), $D_{\text{ax},i}$ and $D_{\text{rad},i}$ are, respectively, the axial and radial dispersion coefficient (m^2/s), $k_{g,i}$ is the external mass transfer coefficient (m/s), a_v is the specific area of the catalyst (m^2/m^3).

On the left hand side of Eq. (1) are represented the terms corresponding to the evolution of the concentration of the species i towards time and the mass transfer of species i in the volume. Due to the permeation phenomena, the radial mass transfer cannot be neglected. On the right hand side are represented the mass transfer of species i in the volume due to axial/radial dispersion and the mass transfer of species i from the gas phase to the catalyst surface. The velocity field is obtained by means of Navier Stokes equations, considering that porous media has average values of porosity ε and permeability κ on the cell. Radial voidage profile is estimated by the empirical correlation of Hunt and Tien [10].

The mass balance on the surface of the catalyst considers that the evolution of the concentration of species i at the surface of the catalyst is a balance between the flux of species coming from the gas phase and the flux of species i consumed by the reactions (Eq. (2)).

$$\frac{\partial C_i^*}{\partial t} - k_{g,i}a_v\left(C_i^{\text{lumen}} - C_i^*\right) = (1-\varepsilon)\quad\rho_p R_i \quad (2)$$

where C_i^* is the concentration of species i at the surface of the catalyst (mol/m^3), ρ_p is the density of the catalyst (kg/m^3), R_i is the total flux of species i consumed by the reactions (mol/kg catalyst/s).

R_i can be linked to the fluxes of species i consumed by each specific reaction j ($r_{s,j}$) by means of:

$$R_i = \sum_{j=1}^{\text{nb\_reactions}} \nu_{i,j} r_{s,j} \tag{3}$$

where $\nu_{i,j}$ is the stoichiometric coefficient of species i in the reaction j and $r_{s,j}$ is the flux of species i consumed by reaction j (mol/kg catalyst/s). Considering that the thermodynamic equilibrium has been reached for each reaction, $r_{s,j}$ can be written under the form below where K_j is the equilibrium constant and k_j the kinetics constant (k_j is assumed to be high enough so that thermodynamic equilibrium is reached).

$$r_{s,j} = k_j \left(\prod_{i=1}^{nb_{\text{reagents}}} C_i^{\text{lumen}\left|\nu_{i,j}\right|} - \frac{1}{K_j} \prod_{k=1}^{nb_{\text{products}}} C_k^{\text{lumen}\left|\nu_{k,j}\right|} \right)$$

3.2. Mass balance in the shell

For each species i, the mass balance is represented in the gas phase by:

$$\frac{\partial C_i^{\text{shell}}}{\partial t} + \left(v_r \frac{\partial C_i^{\text{shell}}}{\partial r} + v_z \frac{\partial C_i^{\text{shell}}}{\partial z} \right) = \frac{\partial}{\partial z}\left(\mathcal{D}_i^m \frac{\partial C_i^{\text{shell}}}{\partial z} \right) + \frac{1}{r}\frac{\partial}{\partial r}\left(\mathcal{D}_i^m \frac{\partial C_i^{\text{shell}}}{\partial r} \right) \tag{4}$$

where C_i^{shell} is the concentration of species i in the shell (mol/m^3), v_r and v_z are, respectively, the radial and axial velocity (m/s), D_i^m is the diffusion coefficient of species i in the mixture (m^2/s).

On the left hand side of Eq. (4) are represented the terms corresponding to the evolution of the concentration of the species i towards time and the mass transfer of species i in the volume. On the right hand side are represented the mass transfer by diffusion of species i in the volume.

The velocity field is obtained by means of Navier Stokes equations.

3.3. Boundary conditions and initialization

Initial conditions for the systems consider that at $t = 0$, the concentrations are null in the whole volume except at the lumen and shell inlets where the concentrations are, respectively, equal to the composition of the deuterated fluid and the composition of the swamping gas.

The classical Danckwerts boundary conditions are used for the inlet and outlet of the catalytic membrane reactor [11]. Considering that the concentration profile is established at the inlet of the bleedoff tube, that species cannot permeate through the bleedoff tube and through the tap on which the spring is fixed, that the concentration profile in the lumen is axisymmetric and that only hydrogen isotopes can permeate through the membrane, one can established the boundary conditions for the lumen side (see Table 1). The isotope permeation flux density (J_i^{memb} mol/m^2/s) through the membrane is equal to zero for all species except for the hydrogen isotopes for which the following equation is used (Richardson law [12]):

$$J_i^{\text{memb}} = \frac{\phi_i}{2\delta}\left(\sqrt{P_i^{\text{lumen}}} - \sqrt{P_i^{\text{shell}}} \right) \tag{5}$$

where δ is the membrane thickness (m), P_i^{lumen} and P_i^{shell} are, respectively, the partial pressure of species i in the lumen and in the shell (Pa) and ϕ_i is the permeability of species i in the membrane (mol/m/s/Pa$^{0.5}$). Note that for HD, the previous equation cannot be used as permeation is a phenomenon which involves atomic species. In the case of *HD*, *H* and *D* have different diffusion coefficients which have an effect on the composition of adsorbed species at the membrane surface before recombination. Hence, for the *HD* permeation flux density, it is proposed to use the following equation [13,14]:

$$J_{HD}^{\text{perm}} = \sqrt{4 J_{H_2}^{\text{memb}} J_{D_2}^{\text{memb}}} \tag{6}$$

Table 1
Boundary conditions for the lumen side.

Domain	Boundary condition
$z = 0 \quad \forall r \in [r_{\text{bleedoff}}; r_{\text{memb}}]$	$C_i^{\text{lumen}} = C_i^{\text{inlet}}$
$z = L_{\text{bleedoff}} \quad \forall r \in [0; r_{\text{bleedoff}}]$	$\left(\partial C_i^{\text{lumen}}/\partial z\right) = 0$
$r = r_{\text{bleedoff}} \quad \forall z \in [0; L_{\text{bleedoff}}]$	$u_r C_i^{\text{lumen}} - \varepsilon \mathcal{D}_{\text{rad},i}\left(\partial C_i^{\text{lumen}}/\partial r\right) = 0$
$z = L_{\text{memb}} \quad \forall r \in [0; r_{\text{memb}}]$	$u_z C_i^{\text{lumen}} - \varepsilon \mathcal{D}_{\text{ax},i}\left(\partial C_i^{\text{lumen}}/\partial z\right) = 0$
$r = 0 \quad \forall z \in [L_{\text{bleedoff}}; L_{\text{memb}}]$	$\left(\partial C_i^{\text{lumen}}/\partial r\right) = 0$
$r = r_{\text{memb}} \quad \forall z \in [0; L_{\text{memb}}]$	$u_r C_i^{\text{lumen}} - \varepsilon \mathcal{D}_{\text{rad},i}\left(\partial C_i^{\text{lumen}}/\partial r\right) = J_i^{\text{memb}}$

Considering that the concentration profile is established at the outlet of the shell, that species cannot permeate through the wall of the shell and through the tap on which the spring is fixed and that only hydrogen isotopes can permeate through the membrane, one can establish the boundary conditions for the shell side (see Table 2 below):

Table 2
Boundary conditions for the shell side.

Domain	Boundary condition
$z = L_{\text{memb}} \quad \forall r \in [r_{\text{memb}}; r_{\text{shell}}]$	$C_i^{\text{shell}} = C_i^{\text{shell}}$
$z = 0 \quad \forall r \in [r_{\text{memb}}; r_{\text{shell}}]$	$\left(\partial C_i^{\text{shell}}/\partial z\right) = 0$
$r = r_{\text{shell}} \quad \forall z \in [0; L_{\text{shell}}]$	$v_r C_i^{\text{shell}} - \mathcal{D}_i^m\left(\partial C_i^{\text{shell}}/\partial r\right) = 0$
$r = r_{\text{memb}} \quad \forall z \in [0; L_{\text{memb}}]$	$v_r C_i^{\text{shell}} - \mathcal{D}_i^m\left(\partial C_i^{\text{shell}}/\partial r\right) = -J_i^{\text{memb}}$

3.4. Parameters

Considering that the thermodynamic equilibrium is reached for all chemical reactions, equilibrium constants for reaction (R1)–(R3) were estimated using a thermodynamic approach.

Assuming ideal gas equation of state and a generic reaction $\upsilon_a A + \upsilon_b B \rightleftharpoons \upsilon_c C + \upsilon_d D$, the equilibrium constant can be estimated by:

$$K = \prod_{i=a}^{d} P_i^{\nu_i} = \exp\left(-\frac{\Delta_r g^0(T)}{RT} \right) \tag{7}$$

The reaction free enthalpy $\Delta_r g^0(T)$ $\left(\text{J/mol}\right)$ is defined as [15]:

$$\Delta_r g^0(T) = \Delta_r h^0(T) - T\Delta_r s^0(T)$$

With:

- $\Delta_r h^0(T) = \Delta_r h^0(T_{\text{ref}}) + \int_{T_{\text{ref}}}^{T} \sum_i \nu_i Cp_i(T)\,\mathrm{d}T$

- $\Delta_r h^0(T_{\text{ref}}) = \sum_{\text{i}} \nu_{\text{i}} \quad \Delta_r h^0_{f,i}(T_{\text{ref}})$

And:

- $\Delta_r s^0(T) = \Delta_r s^0(T_{\text{ref}}) + \int_{T_{\text{ref}}}^{T} \sum_i \frac{\nu_i Cp_i}{T} \mathrm{d}T$
- $\Delta_r s^0(T_{\text{ref}}) = \sum_{\text{i}} \nu_i \quad s_i^0(T_{\text{ref}})$

In the previous equations, $\Delta_r h^0(T)$ is the standard enthalpy of reaction (J/mol) at temperature T, $\Delta_r h^0_{f,i}(T_{\text{ref}})$ is the standard enthalpy of formation of species i at T_{ref} (J/mol), Cp_i is the specific heat capacity of species i (J/mol/K), $\Delta_r s^0(T)$ is the standard entropy of reaction (J/mol/K) at temperature T and $s_i^0(T_{\text{ref}})$ is the entropy of species i at temperature T_{ref} (J/mol/K).

Thermophysical properties required for the estimation of the equilibrium constants can be found in the DIPPR801 Database from AIChE and NIST database. This leads to the following evolution of the equilibrium constants with temperature (Fig. 2).

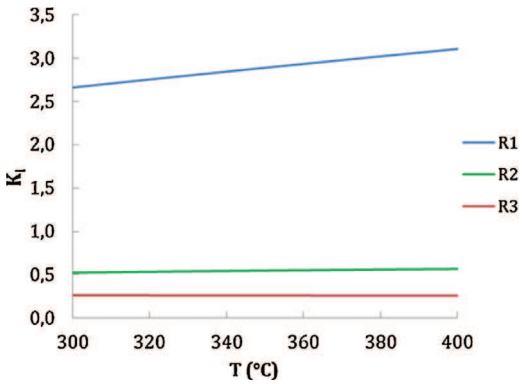

Fig. 2. Equilibrium constants evolution with T.

The permeabilities of protium and deuterium in the membrane were determined in a previous study [9] and are given in the Table 3 below.

Table 3
Permeabilities of H and D in $Pd_{77}Ag_{23}$ membrane.

Species i	Permeability ϕ_i (mol/m/s/Pa$^{0.5}$)
H	$6.1210^{-8}\exp\left(-\left(6876/RT\right)\right)$
D	$4.9310^{-8}\exp\left(-\left(7965/RT\right)\right)$

The other parameters were estimated using correlations established in former studies (see Table 4).

Table 4
Mass transfer parameters.

Parameter	Reference
$\mathcal{D}_i^m$ (non polar mixture)	Chapman-Enskog [16]
$\mathcal{D}_i^m$ (polar mixture)	Brokaw [17]
$\mathcal{D}_{\text{ax},i}$ and $\mathcal{D}_{\text{rad},i}$	Gunn [18]
$k_{g,i}$	Yoshida et al. [19]

4. Modeling assessment

The partial differential equations system defined in Section 3 was implemented in COMSOL Multiphysics®4.3a commercial code and resolved by PARDISO solver. Results of the simulation were compared to experimental results obtained on the facility described in Section 2. Experiments were performed at 320 °C for several compositions of the feed stream composed of nitrogen and D_2O in the range of 0.1 to 4 molar%. The feed stream and swamping gas flowrates were 100 N ml/min. The lumen and shell pressures were, respectively 2.5 bar and 0.5 bar. For each experiment, the dedeuteration factor (DF) was determined as the ratio of the amount of deuterium in the feed stream to the amount of remaining deuterium leaving the lumen [20]. Fig. 3 presents the modeling results in red and the experimental ones in blue bullets.

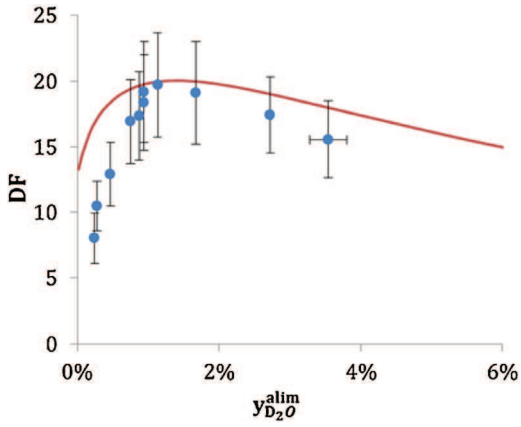

Fig. 3. Evolution of the dedeuteration faction.

The evolution of the DF with the D_2O amount in the feed steam shows a maximum at nearly 1.5 molar% of D_2O. The increase of DF when D_2O amount increases could not be easily foreseen without detailed knowledge of the phenomena occurring in the catalytic membrane reactor. But it can be noted that the model results present a good agreement with experimental measurements.

The evolution of DF could not be interpreted without the gaseous streams compositions measurements or estimations. Fig. 4 shows the evolution of the relative amounts of deuterated species in the lumen output (compared to deuterated species amount in the lumen input) versus the amount of D_2O in the feed stream.

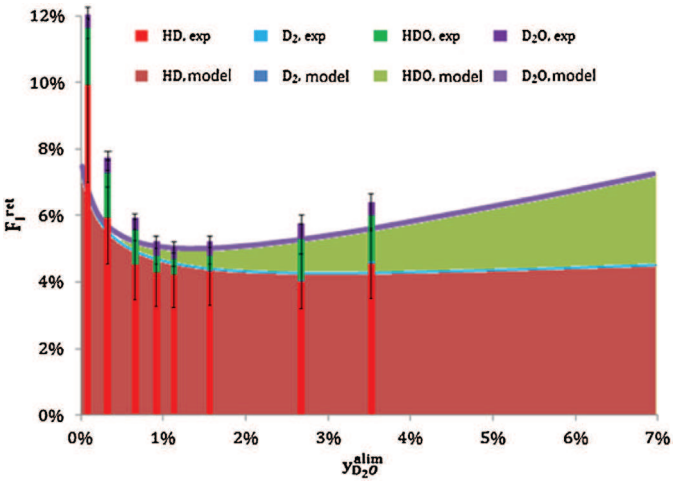

Fig. 4. Evolution of lumen output composition (bar graphs are experimental values; areas are model results).

Below 1.5 molar% D_2O in the feed stream, only few amounts of HDO or D_2O remain in the lumen at the output of the reactor indicating an efficient conversion of D_2O. In the meantime, the relative amount of HD at the output of the lumen decreases with an increase of the D_2O input. This can be explained by an increase of the HD permeation flux as the partial pressure of HD coming from D_2O conversion increases in the lumen. The combination of the improvement of the HD permeation and the efficient conversion of D_2O leads to an improvement of DF as shown on Fig. 3.

Above 1.5 molar% D_2O in the feed stream, the presence of HDO at the output of the lumen increases significantly indicating a depletion of D_2O conversion leading to a decrease of DF (see Fig. 3). It is then clearly demonstrated that above 1.5 molar% D_2O in the feed stream, the permeation flux of hydrogen is not sufficient enough to allow a full conversion of D_2O and that an increase of the partial pressure of hydrogen in the shell side will be necessary to improve the catalytic membrane reactor efficiency.

Finally, the comparison between experimental results and model ones on Figs. 3 and 4 shows the good predictive ability of the model.

5. Conclusion

In this paper, a new 2D modeling approach is proposed to represent the behavior of a catalytic membrane reactor including the estimation of the lumen and shell outputs composition.

The comparison of the model prediction with experimental data have shown a good agreement and the gas phases speciation estimation permits to interpret non trivial behavior of the catalytic membrane reactor. In the next future, further sensitivity analysis will be performed to determine the limits of the model and a kinetics study will be conducted to assess the thermodynamic equilibrium of reactions. However, the model proposed seems already very promising.

References

[1] S. Rosanvallon, et al., ITER waste management, Fusion Eng. Des. 85 (2010) 1788–1791.
[2] A.C. Bell, et al., Detritiation process needed for JET operation and their wider applicability, Fusion Sci. Technol. 41 (2002) 626–631.
[3] L. Dörr, et al., A decade of tritium technology development and operation at Tritium Laboratory Karlsruhe, Fusion Sci. Technol. 54 (2008) 143–148.
[4] K. Liger, et al., Preliminary results from a detritiation facility dedicated to soft housekeeping waste and tritium valorization, Fusion Eng. Des. 89 (2014) 2103–2107.
[5] A. Santucci, et al., Computation and comparison of Pd-based membrane reactor performances for water gas shift reaction and isotope swamping in view of highly tritiated water decontamination, Fusion Eng. Des. 88 (2013) 2413–2416.
[6] K. Munakata, et al., Numerical simulation of membrane reactor for detritiation of plasma exhaust gas, Fusion Sci. Technol. 48 (2005) 17–22.
[7] K. Munakata, D. Demange, Development of numerical simulation code of membrane reactor for detritiation, Fusion Eng. Des. 86 (19–11) (2011) 2334–2337.
[8] S. Tosti, V. Violante, Numerical approach for a study of the hydrogen isotopes separation by palladium alloy membranes, Fusion Eng. Des. 43 (1998) 93–100.
[9] J. Mascarade, et al., On the study of catalytic membrane reactor for water detritiation: membrane characterization, Fusion Eng. Des. 88 (2013) 844–848.
[10] M.L. Hunt, C.L. Tien, Non Darcian flow, heat and mass transfer in catalytic packed bed reactors, Chem. Eng. Sci. 45 (1990) 55–63.
[11] P. Danckwerts, Continuous flow systems—distribution of residence times, Chem. Eng. Sci. 2 (1953) 1–13.
[12] R.E. Buxbaum, A.B. Kinney, Hydrogen transport through tubular membranes of palladium-coated tantalum and niobium, Ind. Eng. Chem. Res. 35 (1996) 530–537.
[13] K. Kizu, T. Tanabe, Deuterium permeation through metals under hydrogen counter flow, J. Nucl. Mater. 1 (1999) 561–565.
[14] K. Kizu, et al., Co-permeation of deuterium and hydrogen through Pd, J. Nucl. Mater. 289 (2001) 291–302.
[15] E. Keszeï, Chemical Thermodynamics: An Introduction, Springer, Berlin, 2012.
[16] S. Chapman, T.G. Cowling, The Mathematical Theory of Non-Uniform Gases, Cambridge University Press, London, 1970.
[17] R.S. Brokaw, Predicting transport properties of dilute gases, Ind. Eng. Chem. Process Des. Dev. 8 (1969) 240–253.
[18] D.J. Gunn, Axial and radial dispersion in fixed beds, Chem. Eng. Sci. 42 (1987) 363–373.
[19] F. Yoshida, et al., Temperatures and partial pressures at the surfaces of catalyst particles, AIChE J. 8 (1962) 5–11.
[20] J. Mascarade, et al., Membrane reactor for water detritiation: a parametric study on operating parameters, Fusion Sci. Technol. 67 (2015) 463–466.